Proposal for CLAS approved analyses

# Deep Virtual Compton Scattering at 4 GeV to 5 GeV with CLAS

H. Aznauryan, N. Dashyan, K. Egiyan
Yerevan Physics Institute, Yerevan, Armenia 375036

V. Burkert[1], M. Ito, E. Smith, Yu. Sharabian
TJNAF, Newport News, VA 23606, USA

H. Egiyan
College of Willam and Mary, Williamsburg, VA 23187, USA

M. Guidal, J.-P. Didelez, E. Hourany, C. Hadjidakis, S. Bouchigny
Institut de Physique Nucleaire, Orsay, France F-91406

R. Miskimen
University of Massachusetts, Amhest, MA 01003, USA

C. Hyde-Wright
Old Dominion University, Norfolk, VA 23529, USA

P. Bertin
University Blaise Pascal/IN2P3, France

P. Stoler
Rensselaer Polytechnic Institute, Troy, NY 12181, USA

J. Ball, D. Doré, M. Garçon, L. Morand, F. Sabatié
CEA-Saclay, Gif-Sur-Yvette Cedex, France F-91191

L. Elouadrhiri[1], S. Stepanyan [1,2], J. Hardie
Christopher Newport University, Newport News, VA 23606, USA

**Abstract**

We propose to study Deep Virtual Compton Scattering (DVCS) using CLAS electroproduction data on hydrogen with 4+ GeV polarized beams. These analyses will include data from runs with already approved beam time.

The main focus of these studies will be the measurements of Beam Spin Asymmetry (or Single Spin Asymmetry, SSA) in the reaction $\vec{e}p \rightarrow ep\gamma$ . SSA is directly proportional to the imaginary part of the DVCS amplitude and it gives access to the Generalized Parton Distributions (GPDs), $H$, $E$. Expected asymmetry from the leading order calculation is 40%. The dependence of the magnitude of SSA on $Q^2$ and $x_B$ will be a good test for the Bjorken regime.

[1]Co-spokesperson
[2]Contact person

The preliminary analyses of CLAS electroproduction data with 4.2 GeV polarized beam shows a clear asymmetry in the $\phi_{\gamma^*\gamma}$ dependence. This is the first observation of DVCS process at JLAB.

# 1 Introduction

One of the fundamental topics of modern high energy physics is the understanding of the nucleon structure. Studies with leptonic beams in the deep inelastic scattering region (DIS) led to discovery of the quark-gluon structure of the nucleon. It was found, for example, that quarks carry about half of the nucleon momentum, and about 25% of the nucleon spin.

To have a more complete picture of nucleon structure new information is needed, particularly, the information on quark-quark and quark-gluon interactions in the nucleon. Recent developments in the theory showed that such information can be obtained in hard exclusive leptoproduction experiments. A formalism, developed by Ji [1], Radyushkin [2] and others, for the QCD description of hard exclusive reactions introduces new Generalized Parton Distributions, GPDs (or Skewed Parton Distributions, or Off-Forward Parton Distributions) that contain information on the interference between different quark configurations on transverse and angular momentum distributions, and provide a unified description of a wide range of inclusive and exclusive reaction.

A broad program for studying GPDs is proposed on CLAS at CEBAF-12 [3]. Although more favorable kinematical conditions for these studies will be reached with a 12 GeV machine, there are measurements that can be done and are very important to do at lower energies as well.

One of the key experiments in the GPD program is Deep Virtual Compton Scattering (DVCS). There are indications that in the case of DVCS the scaling regime may be reached at $Q^2 \sim 2$ (GeV/c)$^2$ (see discussion below). This can be tested with already available data from CLAS.

Currently, a considerable amount of data is on tape from 4+ GeV electron running. The open acceptance of CLAS and the use of a single electron trigger ensures recording of data for all possible final states. In the frame of this work we will analyze all existing electroproduction data from CLAS obtained with 4+ GeV polarized electron beams (CLAS/E1c and E1d). The main focus will be the study of Single Spin Asymmetry (SSA) in the reaction $\vec{e}p \rightarrow ep\gamma$ .

It has been shown that in the leading-order pQCD the amplitude of Deep Virtual Meson Production with longitudinally polarized photons and the amplitude of Deep Virtual Compton Scattering (generally called Deep Exclusive Scattering, DES), in the forward direction can be factorized into a hard-scattering part (exactly calculable in pQCD), and a non-perturbative nucleon structure part as illustrated in Figure 1.

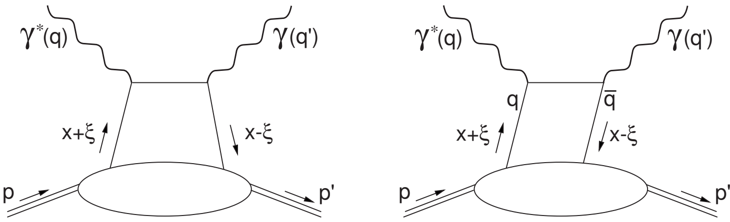


(a) (b)

Figure 1: Hand bag diagrams corresponding to the virtual Compton scattering. Diagram $(a)$ when $\xi$ is greater than $x$ and $(b)$ $\xi$ is less than $x$.

In these so-called "handbag" diagrams, the lower blob represents the structure of the nucleon and can be parameterized in terms of four functions, known as the GPDs.

The GPDs are defined as $H, \tilde{H}, E,$ and $\tilde{E}$, and depend upon three kinematic variables: $x$, $\xi$, and $t$. $x$ is the averaged momentum fraction of the struck quark in the quark loop and, as such, is not directly accessible experimentally. $\xi$ is the longitudinal-momentum fraction of the transfer $\Delta$: in the Bjorken limit, $\xi = x_B/(2 - x_B)$, with $x_B$ the usual Bjorken variable. $t = \Delta^2$ is the standard momentum transfer between the virtual and the real photons.

$H$ and $E$ are spin-independent and $\tilde{H}$ and $\tilde{E}$ are spin-dependent functions. More precisely, the light-cone matrix element of the bilocal quark operator that enters in these hard-electroproduction reactions (represented by the lower blobs in Fig. 1) is at leading twist in $Q^2$ given by:

$$
\begin{aligned}
&\frac{P^+}{2\pi} \int dy^- e^{ixP^+y^-} \langle p'|\bar{\Psi}_\beta(-\tfrac{y}{2})\Psi_\alpha(\tfrac{y}{2})|p\rangle \Big|_{y^+=\vec{y}_\perp=0} \\
&= \tfrac{1}{4}\Big\{(\gamma^-)_{\alpha\beta}\Big[H^q(x,\xi,t)\ \bar{N}(p')\gamma^+N(p) \ +\ E^q(x,\xi,t)\ \bar{N}(p')i\sigma^{+\kappa}\tfrac{\Delta_\kappa}{2M_N}N(p)\Big] \\
&+(\gamma_5\gamma^-)_{\alpha\beta}\Big[\tilde{H}^q(x,\xi,t)\ \bar{N}(p')\gamma^+\gamma_5N(p) \ +\ \tilde{E}^q(x,\xi,t)\ \bar{N}(p')\gamma_5\tfrac{\Delta^+}{2M_N}N(p)\Big]\Big\}\ . \qquad (1)
\end{aligned}
$$

This formula explicitly shows the vector (axial) nature of the $H$, $E$ ($\tilde{H}$, $\tilde{E}$) GPDs associated or not with the $\gamma_5$ matrix.

The GPDs $H$ and $\tilde{H}$ are generalizations of the parton distributions measured in deep inelastic scattering. In the forward direction (defined by $q = q', t = 0$), $H$ reduces to the quark distribution $q(x)$ and $\tilde{H}$ to the quark-helicity distribution $\Delta q(x)$ measured in deep inelastic scattering. Furthermore, at finite momentum transfer, there are model-independent sum rules that relate the integrals of GPDs to the standard hadronic form factors. Also Ji [1] has shown that the first moment of these GPDs gives access to the sum of the quark spin and the quark orbital angular momentum to the nucleon spin, which may shed light on the "spin-puzzle".

DVCS is the most promising channel for studying GPDs at lower energies and $Q^2$. The dominance of the handbag diagram and the behavior of the reduced forward cross section as a $1/Q^4$ (scaling regime) is expected to be reached at lower $Q^2$ than in

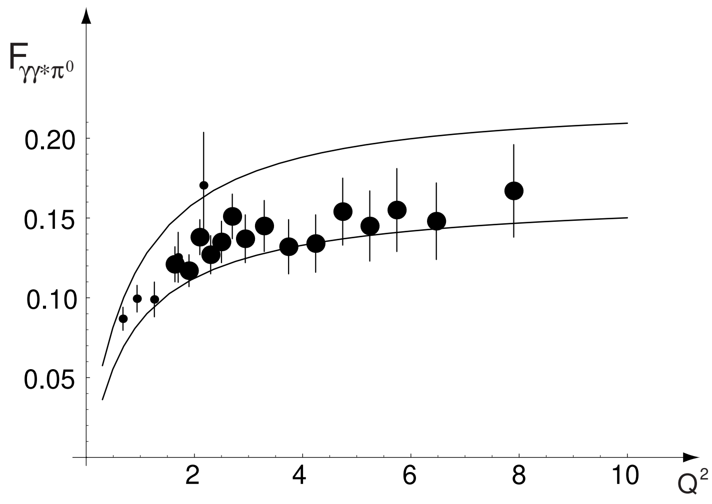


Figure 2: Experimental data on $F_{\gamma^*\gamma\pi^0}$ from [4] with the pQCD predictions using asymptotic shape for the pion distribution amplitude (lower curve) and Chernyak-Zhitnitsky model (upper curve).

the case of deep exclusive meson production. This is supported by measurements of $\gamma^*\gamma\pi^0$ form-factor on $e^-e^+$ colliders. In the leading order pQCD the DVCS process and the production of $\pi^0$ by two photons, where one of the photons is highly virtual, are described according to the same kind of handbag diagram. In Figure 2 the recent measurements of $F_{\gamma^*\gamma\pi^0}$ from CLEO [4] are shown. Curves correspond to the leading order pQCD calculation and to the calculation with power corrections. As it can be seen from the figure $F_{\gamma^*\gamma\pi^0}$ it starts to scale as $1/Q^2$ already at $Q^2 \sim 2$ (GeV/c)$^2$ $-3$ (GeV/c)$^2$. When accounting for the internal quark motion the data are well described for $Q^2 > 1$ (GeV/c)$^2$.

In the experiment one measures DVCS in the interference with Bethe-Heitler (BH) process (see Figure 3). The measured cross section of the reaction $ep \rightarrow ep\gamma$ is a squared sum of DVCS and BH amplitudes:

$$\frac{d^5\sigma}{dQ^2 dx_B dt d\phi} \propto |T^{VCS} + T^{BH}|^2 \tag{2}$$

The DVCS contributions can be extracted from measurements in various ways:

- Direct measurements of the modulus of the DVCS amplitude in regions where the BH contribution is small.
- Accessing the interference between the DVCS and BH amplitudes; in particular the use of a longitudinally polarized electron beam yields the determination of the Single Spin Asymmetry (SSA), directly proportional to the imaginary part of $T^{VCS}$.

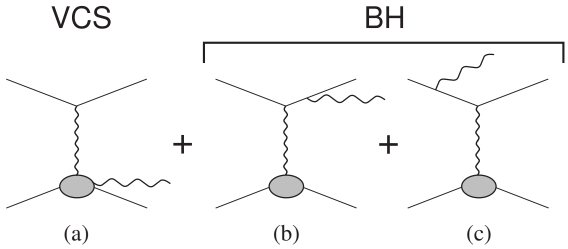


Figure 3: Feynman diagrams for VCS and Bethe-Heitler processes contributing in the amplitude of $ep \to ep\gamma$ scattering.

- Accessing the real part of the DVCS amplitude by measuring the beam charge asymmetry ($e^-$ and $e^+$ beams)

At low energies the BH amplitude dominates while with increasing beam energy the relative strength of DVCS increases (see Figure 4), and is predicted to become the dominant contribution at very high energies. It is clear from Figure 4 that at energies of 4 GeV to 6 GeV, the BH contribution is dominant. Therefore in the framework of this proposal only SSA can be studded. Kinematical range accessible at these beam energies is $Q^2$ from 1 (GeV/c)$^2$ to 4 (GeV/c)$^2$, $x_B$ from 0.2 to 0.5 and the transferred momentum $t$ up to 1 (GeV/c)$^2$ (see Figure 5).

The availability of highly polarized electron beam will allow the measurement of Single Spin Asymmetry (SSA). The asymmetry arises as a result of an interference between real and imaginary parts of longitudinal and transverse amplitudes.

The difference of differential cross sections of $\vec{e}p \to ep\gamma$ at opposite helicities of beam is proportional to the product of imaginary part of the DVCS amplitude and the BH amplitude:

$$\frac{d^5\sigma^+}{dQ^2dx_Bdtd\phi} - \frac{d^5\sigma^-}{dQ^2dx_Bdtd\phi} \sim Im(T^{VCS}) \times T^{BH} \qquad (3)$$

where "+" and "-" denotes positive and negative helicities of the beam. The amplitude of measured asymmetry will be proportional to the magnitude of the imaginary part of the DVCS amplitude. In the first stage of the data analysis the asymmetry $\sigma^+ - \sigma^-/(\sigma^+ + \sigma^-)$ will be more easily obtained than above cross section difference. Its expression in terms of VCS and BH amplitudes is however slightly more complex because of the cross section in the denominator. Following Ref.[6], taking their expression of $|T^{BH}|^2$, $|T^{VCS}|^2$ and interference terms ($INT$) as a function of beam helicity and $\phi$ angle to order $O(1/Q^2)$, and, in addition, only keeping the terms that conserve the photon helicity, the SSA can be expressed as

$$\frac{\sigma^+ - \sigma^-}{\sigma^+ + \sigma^-} = \frac{\frac{1}{Q}B_{INT}\sin\phi + O(\frac{1}{Q^2})}{A_{BH} + \frac{1}{Q}(C_{BH} + C_{INT})\cos\phi + O(\frac{1}{Q^2})} \qquad (4)$$

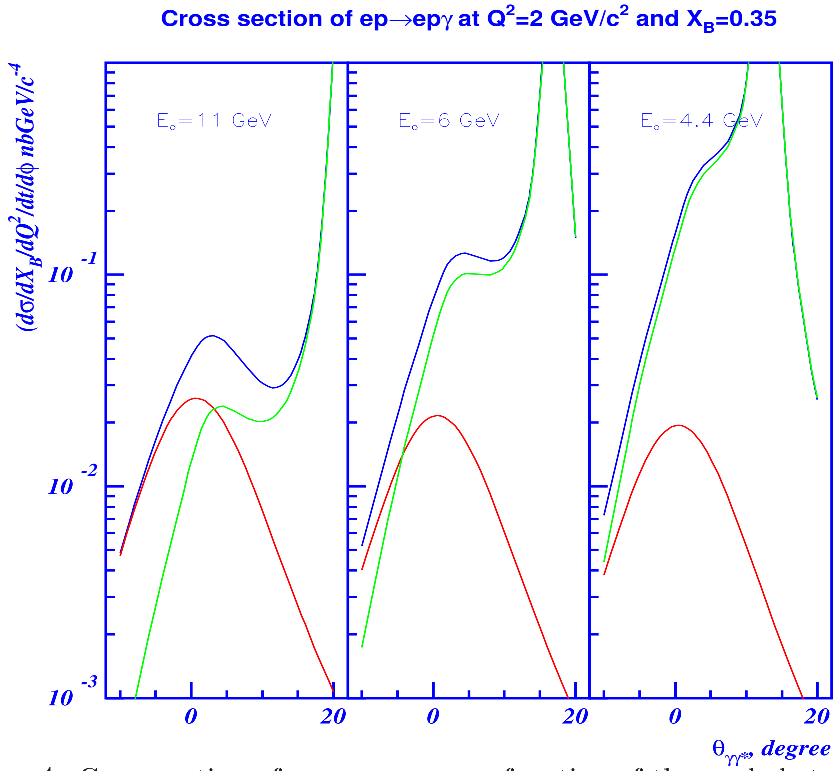


Figure 4: Cross section of $ep \rightarrow ep\gamma$ as a function of the angle between virtual and real photons at beam energies 4.4 GeV, 6 GeV and 11 GeV. Kinematics of the reaction was fixed at $Q^2 = 2\ GeV/c^2$ and $X_B = 0.35$. Red curve is the contribution of DVCS, green curve is Bethe-Heitler and blue curve is the total. Cross sections are calculated according to [5].

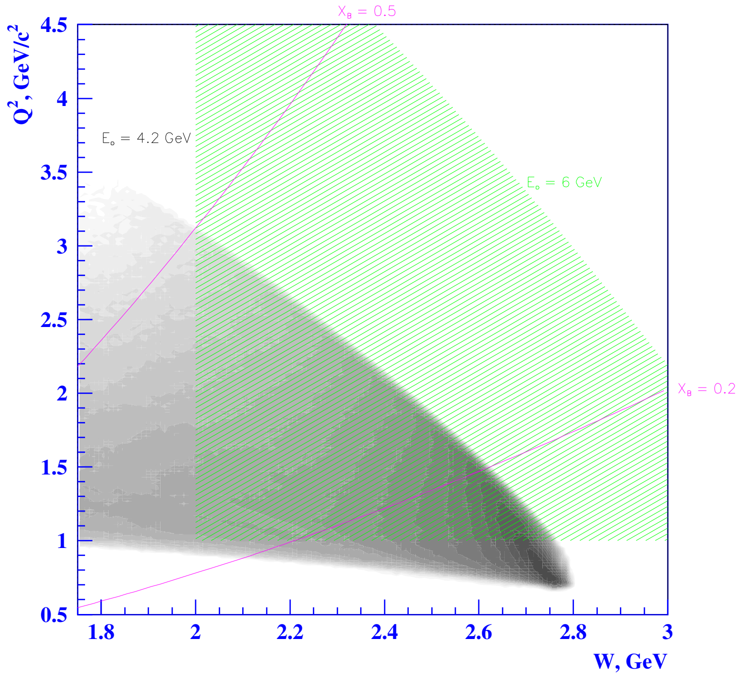


Figure 5: The accessible range of $Q^2$ and $W$. Scattered plot corresponds to kinematics at 4.2 GeV beam energy (from data at torus current 2250A), Filled area is the range accessible with 6 GeV beam. Magenta lines represent fix values of $x_B$.

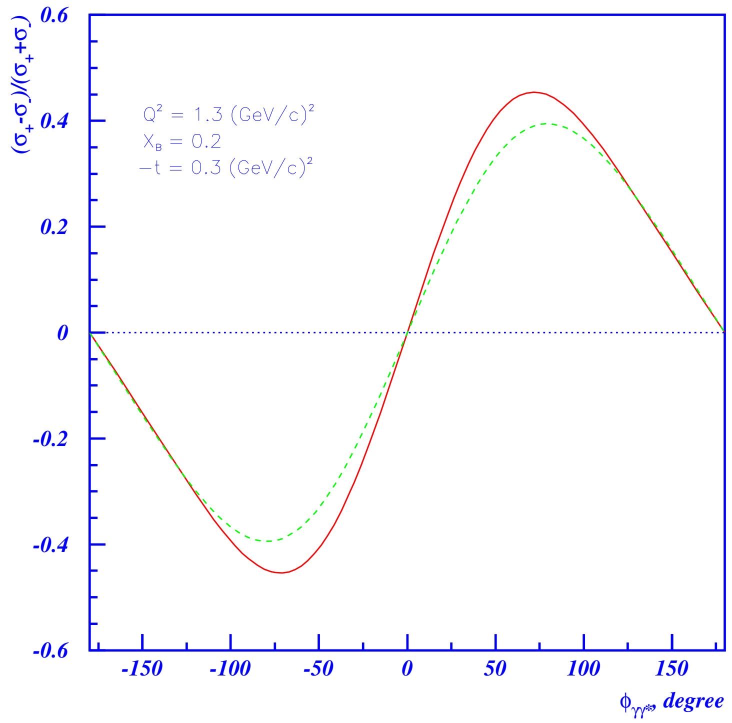


Figure 6: Predicted single spin asymmetry with longitudinally polarized 4.278 GeV electron beam. Kinematics is fixed at $Q^2 = 1.3$ (GeV/c)$^2$, $-t = 0.3$ (GeV/c)$^2$ and $X_B\ = 0.2$. Calculations according [5].

So, in the limit of high $Q$ and photon helicity conserving process (such as the handbag diagram), the dominant feature of the SSA will be a $\sin\phi$ dependence; in addition both the $Im(T^{VCS})$ (in $B_{INT}$) and $Re(T^{VCS})$ (in $C_{INT}$) may be extracted from the $\phi$ distributions.

In Figure 6 the predicted asymmetry at 4.278 GeV beam energy for $Q^2 = 1.3$ (GeV/c)$^2$, $-t = 0.3$ (GeV/c)$^2$ and $x_B\ = 0.2$, is shown. One expects a physical asymmetry of about 40% at this kinematics. The curves correspond to two different model assumptions.

The reaction $ep \ \rightarrow\ ep\gamma$ can be identified through the determination of the missing mass $M_X$ for the detected $(ep\gamma X)$ and $(epX)$ final states. At the kinematics reachable with 4 GeV to 6 GeV electron beams ($\overline{W} \sim 2.5GeV$ and $\overline{Q}^2 \sim 2.GeV/c^2$) the virtual photon direction is about $7^o$ relative to the beam. At small transferred momentum range $-t\ \leq 0.5GeV/c^2$ the angle between virtual and real photons is less than $10^o$. These lead to very small detection acceptance for real photons in the kinematical range of interest at the nominal setting of CLAS. The $ep\ \rightarrow\ ep\gamma$ events are then selected from $ep\ \rightarrow\ epX$ detected configurations

In this configuration the main background to the $ep\ \rightarrow\ ep\gamma$ will be from $ep\ \rightarrow\ ep\pi^0$ . The missing mass squared distributions of $ep\ \rightarrow\ epX$ for both reactions are very close and it will be hard to cleanly separate $\pi^0$'s and photons at high energies and high $W$. In Figure 7 $MM^2(ep\ \rightarrow\ epX\ )$ vs $W$ for events from 4.278 GeV runs at $I_T\ =\ 2250\ A$ is plotted. One can see the pion peak at lower

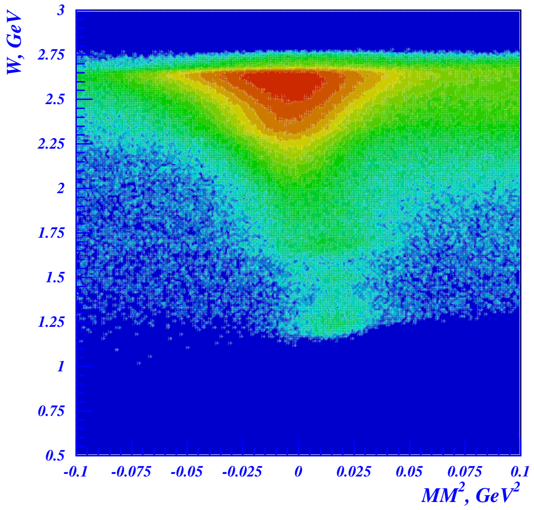


Figure 7: Missing mass vs W for the reaction $ep \rightarrow epX$ at 4.2 GeV beam energy. Events are from runs with torus current $I_T = 2250A$.

$W$, around the delta resonance, but at high $W$ the peaks are broadened due to poor resolution.

Since there is contamination to the final sample of $(ep\gamma)$ events from $(ep\pi^0)$, it is important to estimate the contribution of $\pi^0$ and subtract it from the final sample. This will be done using simulation and two photon $(\pi^0)$ events from the data. In Figure 8 the distribution of missing mass squared of $(epX)$ vs the invariant mass of the detected photons in the reaction $ep \rightarrow ep\gamma\gamma X$ is presented. One can see a nice separation of $(ep\pi^0)$ events.

The data sample from E1c 4.278 GeV runs at $I_T = 2250\ A$ is used to study possible Single Spin Asymmetry in the reaction $\vec{e}p \rightarrow ep\gamma$ . For each selected $(ep)$ event the missing four momentum is calculated. Then missing mass cuts are applied to select the $ep\gamma$ final state from $ep \rightarrow epX$ . In Figure 9 the $MM_X^2$ distribution, green line, with the accepted region, shaded area, is shown. On the plot magenta line corresponds to the missing mass distribution for $ep \rightarrow ep\pi^0$ final state. It is evident that in $ep \rightarrow ep\gamma$ final state is dominant in the selected region.

For final selected events azimuthal and polar angles of the missing photon relative to the virtual photon are calculated. In Figure 10 the ratio of the difference to the sum of the yields of the reaction $\vec{e}p \rightarrow ep\gamma$ for different helicity of incoming electrons is plotted as a function of $\phi_{\gamma^*\gamma}$. These yields are integrated in a wide range of kinematics and are not corrected for pion contamination.

In Figures 11 and 12 the same ratio is shown for different transferred momenta and $x_B$ regions. The ratio is corrected for the beam polarization which was 65%. There is a significant asymmetry for the selected samples, strongly suggestive of a dominant $\sin\phi$ dependence (see Eq.4)

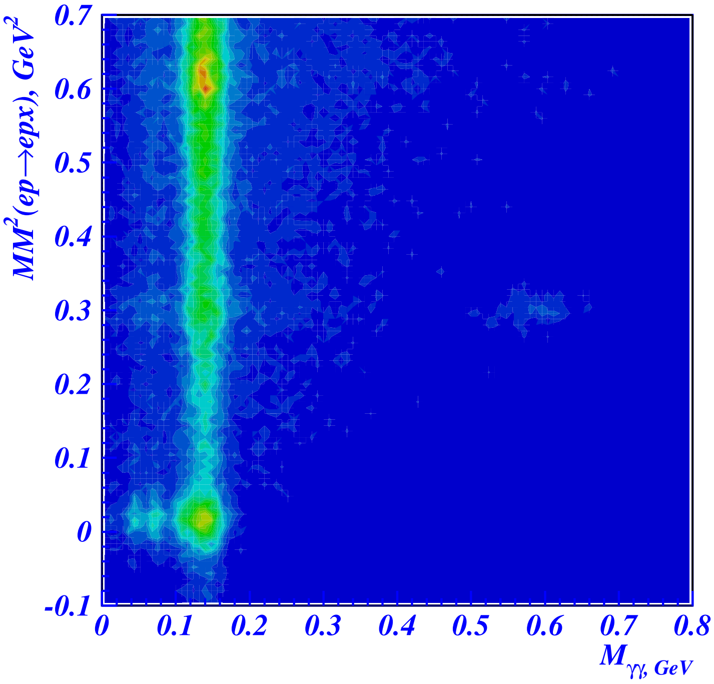


Figure 8: Missing mass vs invariant mass distribution for selected $ep \to ep\gamma\gamma$ events.

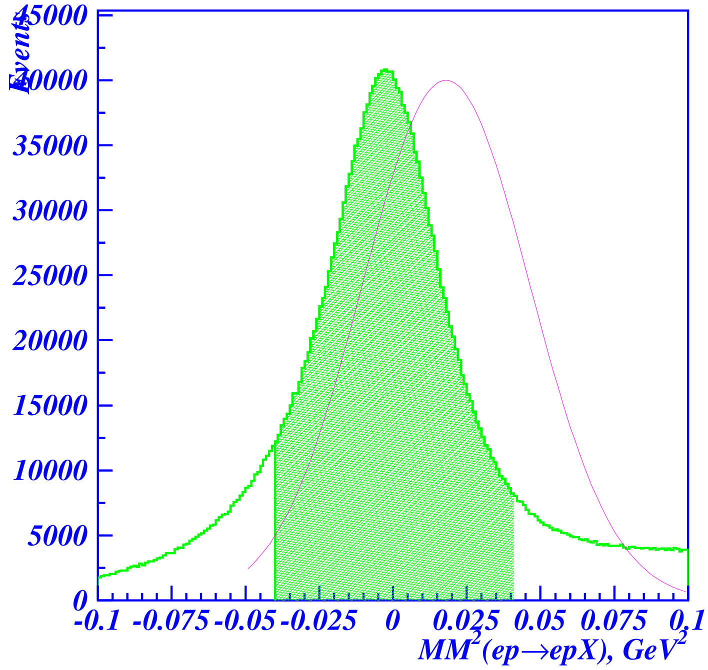


Figure 9: Missing mass distribution in the reaction $ep \to epX$ at $W \geq 2\ GeV$. Shaded region corresponds to selection of $ep\gamma$ final state. On the plot function representing $ep \to epX$ missing mass distribution for the events $ep \to ep\pi^0$ .

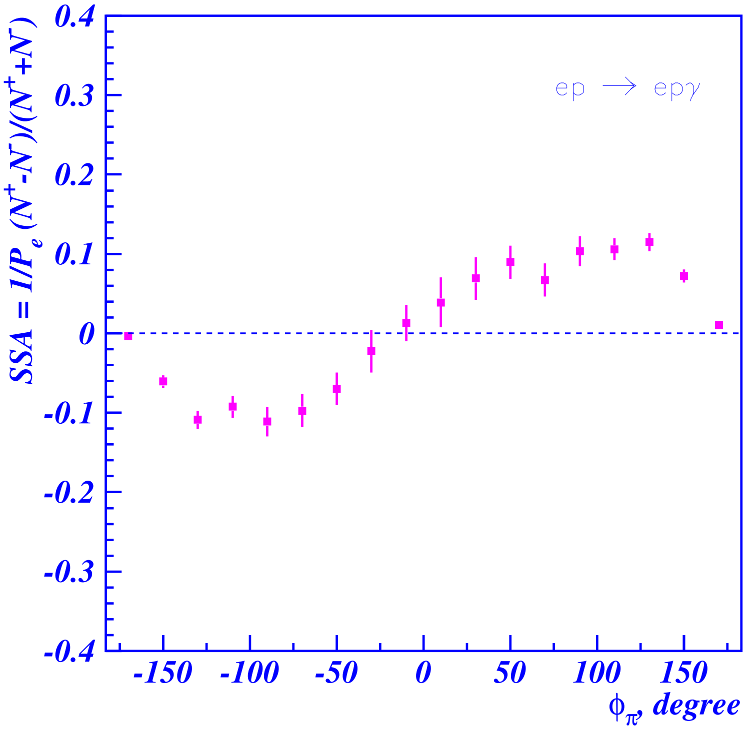


Figure 10: Single Spin Asymmetry extracted from CLAS/E1 data obtained with 4.278 GeV polarized electron beam. Torus current was 2250A. Events are integrated over full range of kinematics at W $\geq$ 2 GeV.

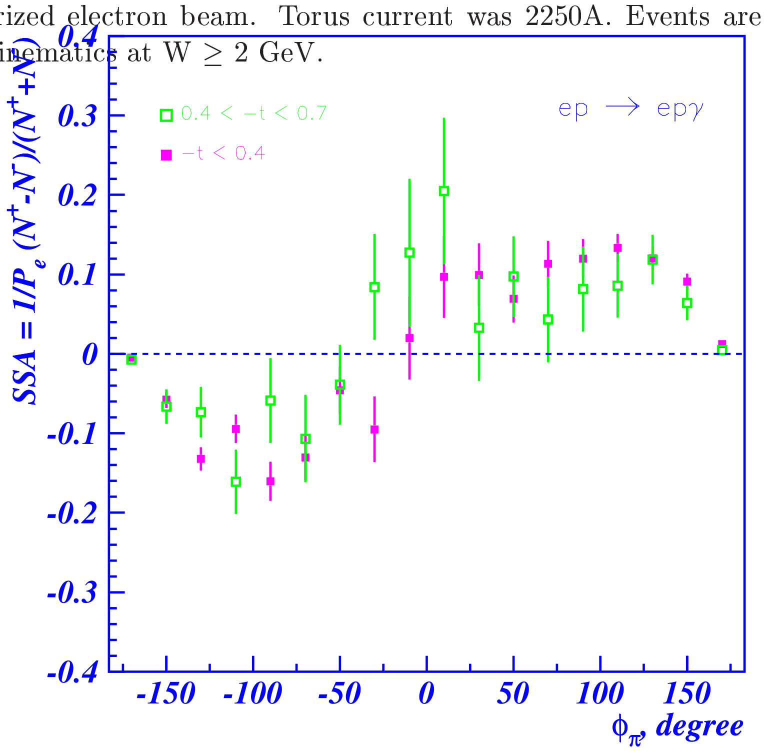


Figure 11: Single Spin Asymmetry extracted from CLAS/E1 data obtained with 4.278 GeV polarized electron beam. Torus current was 2250A. Electron kinematics is fixed at W $\geq$ 2 GeV and $Q^2 \geq 0.8$ $(GeV/c)^2$. Points are for two regions of -t: black squares are -t $\leq$ 0.4 $(GeV/c)^2$ and open squares are 0.4 $(GeV/c)^2 \leq$ -t $\leq$ 0.7 $(GeV/c)^2$.

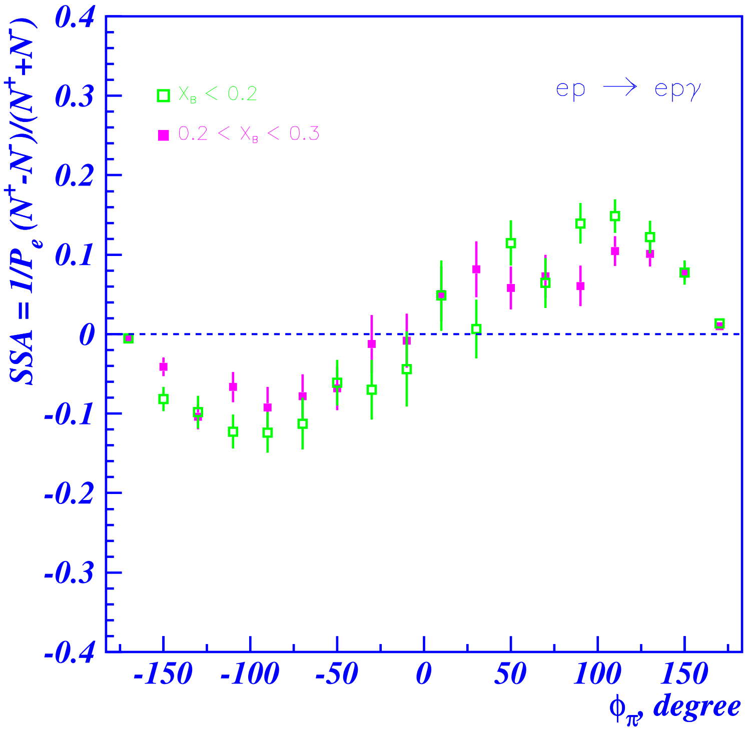


Figure 12: Single Spin Asymmetry extracted from CLAS/E1 data obtained with 4.278 GeV polarized electron beam. Torus current was 2250A. Electron kinematics is fixed at W $\geq$ 2 GeV and $Q^2 \geq 0.8$ $(GeV/c)^2$. Points are for two regions of $X_B$: open squares are for $X_B \leq 0.2$ and filled squares are for $0.2 \leq X_B \leq 0.3$.

In the above selection there are contributions from $ep \rightarrow ep\pi^0$ events. It is important to not only estimate the number of $(ep\pi^0)$ events in the sample but also the contribution to the SSA. In Figure 13 SSA for $\vec{e}p \rightarrow ep\pi^0$ reaction from two gamma events is presented.

The statistical accuracy is low, however there is no visible asymmetry in the $\pi^0$ channel. A fit to the points consistent with "zero" asymmetry ($\chi^2 = 16.9$, $NDF = 17$ and $CL \approx 60\%$). This means that the pion contribution to the SSA of $(ep\gamma)$ enters as a dilution factor and can be taken out after a proper estimation of the $\pi^0$ contribution to the selected $ep \rightarrow epX$ events.

A first look at the E1c data at $E_o = 4.278$ GeV and $I_T = 2250\ A$ shows a clear asymmetry in the reaction $\vec{e}p \rightarrow ep\gamma$ . This sample represents all data at this beam energy and torus setting. Analyzing the remaining "cooked" data from the E1c run period at $E_o = 4.4\ GeV$ and $I_T = 3375\ A$, will increase existing statistics by a factor of two.

Studies will continue with E1d data as soon as that data gets "cooked" (statistics about the same as in E1c).

A simulation in GSIM will be conducted using kinematics of data to estimate the $\pi^0$ contamination in the selected $(ep\gamma)$ final states.

In parallel, the effect of integrating over a wide acceptance will be estimated using

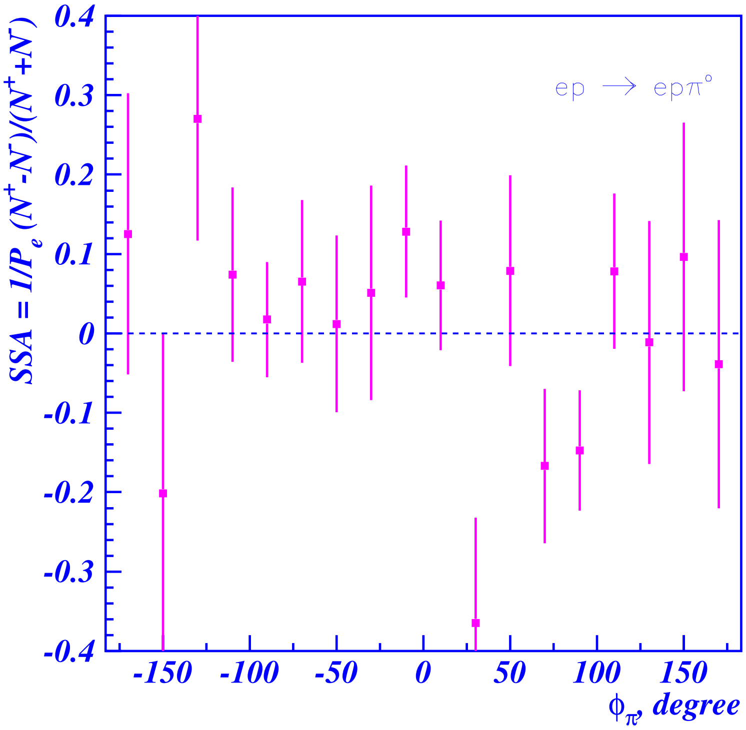


Figure 13: Single Spin Asymmetry for $ep \rightarrow ep\pi^0$ events.

a theoretical model.

The main results of these studies will be mapping out SSA for $\vec{e}p \rightarrow ep\gamma$ in the range of $Q^2$ from 1 $GeV/c^2$ to 4 $GeV/c^2$ and $x_B$ from 0.2 to 0.5. These studies are important for understanding the validity of the scaling regime in DVCS. SSA will be extracted for the $\vec{e}p \rightarrow ep\pi^0$ reaction as well. This will help estimate the residual contribution of $\pi^0$ events in the asymmetry measured for virtual Compton scattering.

# References


[1] X. Ji, Phys. Rev. Lett. **78**, 610 (1997); Phys. Rev. D **55**, 7114 (1997).

[2] A.V. Radyushkin, Phys. Lett. B **380**, 417 (1996); Phys. Rev. D **56**, 5524 (1997).

[3] White Paper CEBAF @ 12 GeV, http://www.jlab.org/div_dept/physics_division/GeV.html.

[4] J. Gronberg et al. (CLEO Collaboration), Phys.Rev. **D 57**, 33 (1998)

[5] M. Vanderhaeghen, M. Guidal and P. Guichon "Computer Code for DVCS and BH Calculations", Private communications.

[6] M. Diehl *et al.*, Phys. Lett. B **411**, 193 (1997).